Atmos. Meas. Tech. Discuss., 5, 8839–8857, 2012
www.atmos-meas-tech-discuss.net/5/8839/2012/
doi:10.5194/amtd-5-8839-2012


Atmospheric Measurement Techniques Discussions



# On the characteristics of ASCAT wind direction ambiguities

**W. Lin[1], M. Portabella[1], A. Stoffelen[2], and A. Verhoef[2]**

[1]Institut de Ciències del Mar (ICM) – CSIC, Barcelona, Spain
[2]Royal Netherlands Meteorological Institute (KNMI), De Bilt, The Netherlands

Received: 23 October 2012 – Accepted: 8 December 2012 – Published: 18 December 2012

Correspondence to: W. Lin (wenminglin@cmima.csic.es)

Published by Copernicus Publications on behalf of the European Geosciences Union.

## Abstract

The inversion of the Advanced Scatterometer (ASCAT) backscatter measurement triplets generally leads to two wind ambiguities with similar wind speed values and opposite wind directions. However, for up-, down- and cross-wind (with respect to the mid beam azimuth direction) cases, the inversion often leads to three or four wind solutions. In most of such cases, the inversion residual or maximum likelihood estimator (MLE) of the 3rd and 4th solutions (i.e. high-rank solutions) are substantially higher than those of the first two (low rank) ambiguities, indicating a low probability of the former and thus essentially dual ambiguity. This paper investigates the characteristics of ASCAT high-rank wind solutions under different conditions with the objective to develop a method for rejecting the spurious high-rank solutions. The implementation of this rejection procedure improves the effectiveness of the ASCAT wind quality control (QC) and ambiguity removal procedures.


## 1 Introduction

The Advanced Scatterometer (ASCAT) is one of the instruments onboard the Metop-A satellite, which is a polar-orbiting meteorological satellite launched on 19 October 2006. It operates at a microwave frequency of 5.255 GHz (C-band), with three vertically polarized fan beams pointing into a swath at each side of the sub-satellite track (Figa-Saldana et al., 2002). A swath consists of a matrix of Wind Vector Cell (WVC) numbered across-track from outer swath to inner swath. An important tool for interpreting the ASCAT data is the visualization of the triple $\sigma^{\circ}$ measurements (named triplet) that correspond to the three antenna beams in the 3-dimensional measurement space at each cross-track WVC (Stoffelen and Anderson, 1997). For a given WVC number, the backscatter signal mainly depends on the sea-surface wind speed and wind direction, since the parameters of geometrical measurement are fixed. In the 3-D-space visualization, ASCAT measured triplets are distributed around a well-defined "conical"





AMTD
5, 8839–8857, 2012

surface. The latter surface is described by the forward model or Geophysical Model Function (GMF), which represents the best fit to the measured triplets. The GMF relates the backscatter measurements to the observing geometry and the mean wind vector in a WVC. The radar antenna geometry, the measurement noise, as well as non-linearities in the GMF complicate the wind retrieval process, which in general leads to several wind vector ambiguities. These ambiguities are generally ranked by their probability or distance to the GMF surface, which is called inversion residual or maximum likelihood estimator (MLE) (Stoffelen and Portabella, 2006). A spatial filter, the so-called ambiguity removal (AR) scheme (Stiles et al., 2002; Vogelzang et al., 2009), is then applied to produce the final or "selected" wind field.

Figure 1 shows the distribution of triplets (points) around a cone cross section (double ellipse), which corresponds to ASCAT WVC number 1. Note that the cross section corresponds to a roughly constant wind speed (e.g. $8\,\mathrm{m\,s^{-1}}$ in Fig. 1) whereas the wind direction varies along the double ellipse, such that the uppermost triplets correspond to winds blowing along the ASCAT mid beam direction (upwind/downwind or $0^\circ/180^\circ$), whereas at the lowest points the wind blows roughly across the mid beam direction (crosswind or $90^\circ/270^\circ$). The wind inversion minimizes the distance between the measured triplet and the cone surface. For triplets lying close to the cone surface, the inversion generally leads to 2 wind solutions or ambiguities $180^\circ$ apart, i.e. two specific locations on the cone surface minimize such distance due to the double-ellipse shape of the GMF. Ambiguity removal is generally not difficult in such cases. In contrast, triplets close to the cone centre (and therefore far from the cone surface) generally lead to 3–4 wind solutions. Such triplets are generally affected by geophysical conditions other than those modelled by the GMF, such as rain, sea ice, confused sea state and local wind variability, thus leading to lower quality wind retrievals. A quality control (QC) scheme is used to detect and filter cases that lead to poor quality retrievals.

Recent research shows that near the up-, down- and cross-wind directions, there is also a substantial number of triplets which lie close to cone, but have more than two solutions (see Fig. 1). Besides the first two wind solutions, which correspond to



AMTD
5, 8839–8857, 2012

the typical dual ambiguities derived from triplets near the cone surface, there is a 3rd and, in some cases, 4th solution typically in between the 1st and 2nd solution (at 90°). A 90° shift in wind direction on the cone surface corresponds to an opposing point, i.e. from up- or downwind to crosswind or vice versa. According to inversion theory, measured triplets close to the solution surface lead to good quality wind retrievals. However, the relevance of the additional 3rd and 4th wind solutions on the opposing side of the cone has never been assessed. That is, are these so-called "high-rank" solutions meaningful in terms of probability of being the true wind or rather artefacts of the inversion procedure?

In Sect. 2, it is shown that some "high-rank" solutions are in fact spurious and should therefore be removed after inversion (before the ambiguity removal step). In Sect. 3, a method to distinguish between the "spurious" high-rank solutions and the more credible high-rank solutions is proposed, and which validation is presented in Sect. 4. Finally, conclusions and recommendations can be found in Sect. 5.

## 2 Scatterometer inversion

Currently, the operational C-band GMF is CMOD5n (Hersbach et al., 2007), which is depicted in $z$-space as follow,

$$z_s(\theta, v, \phi) = B_0(\theta, v)^{0.625} \times [1 + B_1(\theta, v)\cos(\phi) + B_2(\theta, v)\cos(2\phi)] \quad (1)$$

where $\theta$ is the scatterometer incidence angle, $v$ and $\phi$ are the sea-surface wind speed and wind direction w.r.t. radar beam azimuth, respectively. $B_0$ is the dominant term setting the wind speed scale, while $B_1$ and $B_2$ serve to resolve the wind direction. The particular value of $B_0$, $B_1$ and $B_2$ is presented by Verhoef et al. (2008). The most common approach used for scatterometer wind inversion is the maximum likelihood estimator (Cornford et al., 2004; Pierson, 1989; Stoffelen and Anderson, 1997; Stoffelen and Portabella, 2006). For ASCAT, the following Maximum Likelihood Estimator (MLE) function is minimized (Stoffelen and Anderson, 1997),





AMTD
5, 8839–8857, 2012

$$\mathrm{MLE} = \frac{1}{3}\sum_{i=1}^{3}(z_{\mathrm{m}i} - z_{\mathrm{s}i})^2 \tag{2}$$

where $z_{\mathrm{m}i} = (\sigma^{\circ}_{\mathrm{m}i})^{0.625}$ is the backscatter measurement of the $i$th beam in $z$-space, and $z_{\mathrm{s}i} = (\sigma^{\circ}_{\mathrm{s}i})^{0.625}$ is the transformed backscatter simulated through Eq. (1). The inversion can therefore be interpreted as the search for the minimum distance between the triplet and the GMF in a transformed 3-D measurement space, i.e. the minimum distance between the triplet and the cone surface (as illustrated in Fig. 1). The retrieved wind solutions are then sorted by the MLE value, i.e. the first ranked solution corresponds to the lowest MLE value (i.e. shortest distance between the triplet and the cone surface), and so on. Note that the lower the MLE, the higher the probability of being the true wind.

The MLE value is a good indicator of the retrieved wind quality (Portabella and Stoffelen, 2001; Portabella et al., 2012a). To improve the ASCAT MLE-based QC, an MLE sign has been defined by Portabella et al. (2012a) and implemented in the Numerical Weather Prediction (NWP) Satellite Application Facility (SAF) ASCAT Wind Data Processor (AWDP). The sign works as follows: triplets located inside the cone are assigned with a positive MLE value, while those located outside the cone are assigned with a negative MLE value. Note that since the cone surface has two manifolds (as represented by the double-ellipse cross section in Fig. 1), the 1st and 2nd rank ambiguities for a triplet located between the manifolds will have opposite MLE signs, i.e. the triplet will be considered inside (outside) the cone surface for the wind solution lying on the outer (inner) cone manifold.

As discussed in Sect. 1, when the triplets lie close to the cone surface, the inversion typically leads to two wind solutions. The solid line in Fig. 2 illustrates the MLE versus wind direction for one of such cases, in which two well-defined minima with similar and low MLE values, i.e. equally and highly probable solutions, are found. Such triplets generally lead to high-quality winds after AR.

When triplets lie far away from the cone surface (e.g. triplets located near the centre of the cross section in Fig. 1), the inversion leads to typically three or four solutions (Portabella and Stoffelen, 2001) with similar and large MLE values (as illustrated by the dashed line in Fig. 2), i.e. up to 4 equally-likely wind ambiguities. Moreover, for such cases, the minima are less well defined, as indicated by the low wind direction modulation of the dashed curve in Fig. 2 and thus have low quality. This is an indication of enhanced isotropy of ocean backscatter conditions, i.e. reduced wind direction skill, which explains the poor quality wind vector retrieval (Stoffelen and Anderson, 1997).

The dotted line in Fig. 2 presents the wind retrieval for a triplet close to cone surface at up-/down-wind location. There are two well-defined minima and two secondary minima. The former (1st and 2nd ranked solutions) correspond to high-probability (low MLE value) wind solutions at up/downwind directions and the latter (3rd and 4th ranked or high-rank solutions) correspond to low-probability (high MLE value) crosswind solutions. A similar effect occurs with triplets close to crosswind direction. In this case, the well-defined minima (1st and 2nd rank solutions) correspond to crosswind and the secondary minima (high-rank solutions) to up/downwind (not shown in Fig. 2).

According to the shape of the MLE cost function curves in Fig. 2, one can clearly discern two types of distinct behaviour: triplets close to the cone (solid and dotted curves) and triplets far away from the cone (dashed curve). The former, with well-defined minima, produce high-quality winds, whereas the latter, with ill-defined minima, represents lower quality winds, some of which may be rejected. For triplets close to the cone surface at up/downwind and crosswind locations (dotted line), the secondary minima (high-rank solutions) are poorly defined (broad) and of very low probability as compared with the primary (1st and 2nd rank) minima (see large MLE difference between primary and secondary minima in dotted curve). They are actually produced by the particular cone shape at such wind direction locations, which is driven by the GMF sensitivity to wind changes and the ASCAT observing geometry. In other words, it seems that such high-rank solutions are spurious (or meaningless) and should therefore be rejected before the AR step. A method to separate high-rank solutions in case of enhanced ocean





AMTD
5, 8839–8857, 2012

isotropy (i.e. triplets close to the cone centre) from those with nominal anisotropy (i.e. triplets close to the cone surface at up-/down- and cross-wind locations) is therefore required.

## 3 Criterion for rejecting high-rank solutions

To discern the characteristics of ASCAT high-rank ambiguities, three and a half years of Ocean and Sea Ice (OSI) SAF 12.5-km ASCAT level 2 (L2) wind data are firstly collocated with the Tropical Rainfall Measuring Mission's (TRMM) Microwave Imager (TMI) rain data. European Centre for Medium-range Weather Forecasts (ECMWF) winds are also used in the following analysis, which are already collected in the ASCAT L2 Binary Universal Format Representation (BUFR) data. Furthermore, a data set with buoy meansurements is examined. This data set collocates three years (March 2009–February 2012) of OSI SAF 12.5-km ASCAT L2 BUFR data with the wind and precipitation data measured by the tropical moored buoy. The studied buoy data are provided by the National Oceanic Atmospheric Administration (NOAA) Tropical Ocean Atmosphere (TAO) buoy arrays in the tropical Pacific, the Prediction and Research Moored Array in the Atlantic (PIRATA), and the Research Moored Array for African-Asian-Australian Monsoon Analysis and Prediction (RAMA) located in the tropical Indian Ocean.

As initial criterion for the high-rank solution rejection procedure, no rejections are performed for wind retrievals below $4\,\mathrm{m\,s^{-1}}$ and, in contrast, above $4\,\mathrm{m\,s^{-1}}$ rejections are always performed for triplets lying outside the cone, i.e. when the MLE of the 1st and/or 2nd rank are negative (see Sect. 2). At low wind speed conditions, ASCAT (and scatterometers in general) have poor wind direction skill (low anisotropy) and thus no dual-ambiguity high-quality wind direction solutions are expected. On the other hand, for triplets lying outside the cone, the retrieved winds are of high quality, as shown by Portabella et al. (2012a), and should therefore correspond to dual ambiguity cases.

The most challenging part of the algorithm is to discriminate the high-rank solutions in backscatter conditions with enhanced isotropy from conditions with nominal





AMTD
5, 8839–8857, 2012

anisotropy, in particular for triplets inside the cone. For such purpose, the MLE value is used. As discussed earlier in association with Fig. 2, all solutions for triplets near the central axis of the cone have about the same distance from the GMF surface. As triplets reside closer to the cone surface, the distance (MLE) difference between the high-rank solutions and the low-rank (1st and 2nd rank) solutions increases. Figure 3 shows the ratio between the third-ranked and the first-ranked MLE (i.e. $|MLE_3/MLE_1|$) against the vertical position of the triplets with more than two solutions as shown in Fig. 1. The cross markers indicate that one of the first two ranked MLE values is negative, while the dot markers present the results for triplets with positive $MLE_1$ and $MLE_2$ (i.e. triplets inside the cone). Note the clear discrimination of triplets with respect to cone position, which will be further exploited here. A threshold $T$ is set to reject the meaningless high-rank solutions for those wind retrievals with positive $MLE_1$ and $MLE_2$. In summary, the high-rank solutions are rejected for the wind retrievals with first-ranked wind speed $> 4\,\mathrm{m\,s^{-1}}$, according to the below criterion,

$$MLE_1 < 0 \text{ or } MLE_2 \text{ or } \left|MLE_3/MLE_1\right| > T \tag{3}$$

Figure 2 shows that most cases with only two solutions reside near the cone surface. High-rank solutions in case of nominal anisotropy also reside near the cone surface. Therefore, the rank-1 MLE distributions of these two categories are expected to be similar. The threshold $T$ is determined by using this constraint. Figure 4 shows the MLE histogram of the first-rank solutions for two-solution cases at WVC number 1, and a comparison to that of high-rank rejected cases for various thresholds (see legend). The standard deviation between the histogram of two-solution cases and those cases with rejected high-rank solutions is presented in the upper-left corner of Fig. 4 as a function of the threshold. The minimum value, which indicates the best match between the MLE distributions of the two-solution cases and cases with rejected high-rank solutions, is obtained at $T = 40$ for WVC number 1. By compromising the differences of the MLE histograms over diverse WVCs (not shown), a threshold of $T = 40$ is set for the rejection procedure.





AMTD
5, 8839–8857, 2012

Finally, Fig. 5a shows the mean vector root-mean-square (VRMS) difference between the ASCAT retrieved winds and the ECMWF winds, for two-solution cases (solid line), cases with high-rank solutions rejected (dashed line) and kept (cross-marked line). Note that only rain-free cases according to TMI collocations are taken into account. For WVCs located at outer and middle swath region (WVC number 1–30), the wind retrievals with high-rank solutions rejected have similar performance to that of the two-solution cases, which indicates that the proposed procedure does a good job on rejecting meaningless or geometry-related high-rank solutions. However, for inner-swath WVCs (WVC number 31–41), the mean VRMS of rejected cases increases with WVC number at higher rate than the two solutions cases, even if the threshold is enhanced to an extremely high value (not shown). In fact, this increase is mainly due to the poor rejecting performance at low wind speed (e.g. $< 6\,\mathrm{m\,s^{-1}}$) conditions, in which the distribution of the ratio $|\mathrm{MLE}_3/\mathrm{MLE}_1|$ is much broader than the one of outer-swath WVCs.

Figure 5b presents the same as Fig. 5a but using buoy winds instead of ECMWF as reference. Due to the lack of buoy collocations, all the collocations are examined regardless whether they are rainy or rain-free samples. Again the mean VRMS of high-rank rejected cases is comparable with that of two-solution cases, except for the bump around WVC numbers 29–33, which is due to the very low number of collocations with high-rank rejected cases.

## 4 Analysis of the effectiveness of rejecting high-rank solutions

To verify the impact of the high-rank solution rejection procedure on ASCAT wind retrievals, the number of geometry-related high-rank solutions that would be selected by the 2D-Var AR module if they were not rejected is examined. This number divided by the total number of cases with rejected high-rank solutions is denoted by $R_s$. Ideally, 2D-Var AR should only select a geometry-related high-rank solution in very few cases and rather generally “stick” to either the 1st or the 2nd rank solution. For example, if





AMTD
5, 8839–8857, 2012

a local wind direction error of 45 degrees may allow the selection of a high-rank solution, then its probability of occurrence would be 0.3 % in case of a 15 degrees 2D-Var uncertainty and 4.5 % for 22.5 degrees uncertainty. The latter uncertainty may occur for low winds, while the former is more typical for winds of nominal strength. Both TMI rain-free and rainy collocations are studied. Table 1 presents the $R_s$ results for different WVC number and geophysical conditions. It shows that the ratio $R_s$ decreases with increasing wind speed as expected. For inner-swath WVCs, the higher $R_s$ value indicates that it is not easy to figure out the geometry-related high-rank solutions, probably due to increased wind direction uncertainty caused by reduced GMF sensitivity for lower incidence angles.

The rejected high-rank solutions are more likely to be chosen by the AR module of L2 processing in rainy areas, as compared to the rain-free cases. Since ECMWF winds do not resolve wind variability and downdrafts in rainy areas (Portabella et al., 2012b), it is supposed that the inaccurate background winds may lead to the selection of spurious high-rank solutions through the AR processing. In other words, it is important to reject the meaningless high-rank solutions, especially for rainy conditions.

The validation using buoy data is also examined. Within the total of 86 000 collocations, there are 6140 cases with more than two solutions, among which 2959 are rejected according to the procedure in Sect. 3. The $R_s$ value for the buoy collocations is 1.1 % (i.e. 33 cases with rejected high-rank solutions, but which are selected by the AR module). Furthermore, within the $R_s$ determined category, there are 20 cases in which the first two ranked solutions are closer to the collocated buoy wind than the higher ranks. For the other 13 cases, the selected high-rank solutions diverge more than 30 degrees from the buoy wind direction, but are in slightly better agreement with the buoy than the first two solutions. This is an indication of potential rain-contaminated ASCAT winds. Such poor-quality cases should be quality-controlled, i.e. all solutions rejected rather than only the high-rank solutions. In 16.7 % of cases 2D-Var selected a high-rank solution from the cases with kept high-rank solutions. The mean VRMS difference with the buoy winds is then relatively high and 4.45 $\mathrm{m\,s^{-1}}$, as compared to 2.53 $\mathrm{m\,s^{-1}}$





AMTD
5, 8839–8857, 2012

in cases where the first or second-rank solution was selected. In 54.6 % of cases the selected high-rank solution was also the closest one to the buoy.

## 5 Conclusions

In cases where the ocean return is rather isotropic, inversion of ASCAT backscatter triplets results in more than two solutions, i.e. high-rank solutions (up to four) emerge due to reduced wind direction skill (in cases of, e.g. high sub-WVC wind variability, rain contamination, etc.). These cases are well represented through these additional wind direction ambiguities and which need to be kept. On the other hand, for ASCAT measurement triplets located close to the GMF (cone surface), the inversion procedure results in two wind ambiguities, except for triplets located at up-, down- and cross-wind locations. These additional and artificial high-rank solutions appear due to the cone geometry, which is driven by the ASCAT measurement geometry and the GMF sensitivity. To filter out these geometry-related high-rank solutions an MLE-based method is proposed. The rationale is to reject these meaningless high-rank solutions and avoid the selection of "spurious" ambiguities during the quality control and ambiguity removal steps.

The 3rd and 4th rank rejection criteria are the following: (a) no rejections for ASCAT winds below 4 $\mathrm{m\,s^{-1}}$ (since these are generally cases with poor wind direction skill); and for winds above 4 $\mathrm{m\,s^{-1}}$, (b) reject for triplets outside the cone surface; and (c) reject when $|MLE_3/MLE_1| >= 40$, for triplets inside the cone. It is found that the quality (using both ECMWF and buoy winds as reference) of the less ambiguous (with high-rank solutions rejected) WVCs is similar to that of the dual-ambiguity cases, whereas the quality of fully ambiguous (with 3rd and 4th ranks kept) WVCs is much lower, as expected (since they correspond to poor quality cases). However, for inner swath WVCs, where the wind direction skill is somewhat lower, the rejection procedure is less effective, suggesting that no rejections should be performed for such WVCs below 6 $\mathrm{m\,s^{-1}}$.





AMTD
5, 8839–8857, 2012

Rejected high ranks are more likely to be selected by the AR module (denoted as $R_s$ cases) over rainy areas than over dry areas, which suggests a more negative effect of such cases in rainy conditions when not rejected. However, a significant amount of $R_s$ cases show high-rank solutions to be (slightly) closer to buoy data than low-rank solutions. This shows a potential ASCAT rain-contamination effect on ASCAT WVCs. For such cases, a complementary QC is required since the MLE-based QC does not filter them (triplets are close to the cone surface). An alternative QC has been recently presented by Portabella et al. (2012b) with promising preliminary results. However, further work is required to improve ASCAT rain correction and QC under rainy conditions.

In case that more collocations of ASCAT, buoy wind and precipitation data become available, a quantitative study of the impact of rejecting high-rank solutions on both AR and QC in L2 processing will be carried out.

*Acknowledgement.* The work has been funded under the EUMETSAT Ocean and Sea Ice (OSI) Satellite Application Facility (SAF) Associated Scientist project reference CDOP-SG06-VS03. The software used in this work has been developed through the EUMETSAT Numerical Weather Prediction SAF.

## References

Cornford, D., Csató, L., Evans, D. J., and Opper, M.: Baysian analysis of the scatterometer wind retrieval inverse problems: some new approaches, J. Roy. Stat. Soc. B, 66, 609–626, 2004.

Figa-Saldana, J., Wilson, J. J. W., Attema, E., Gelsthorpe, R., Drinkwater, M. R., and Stoffelen, A.: The advanced scatterometer (ASCAT) on Metop: A follow-on for European scatterometers, Can. J. Remote Sens., 28, 404–412, 2002.

Hersbach, H., Stoffelen, A., and De Haan, S.: The improved C-band ocean geophysical model function: CMOD-5, J. Geophys. Res., 112, C03006, doi:10.1029/2006JC003743, 2007.

Pierson, W. J.: Probabilities and statistics for backscatter estimates obtained by a scatterometer, J. Geophys. Res., 94, 9743–9759, 1989.

Portabella, M. and Stoffelen, A.: Rain detection and quality control of SeaWinds, J. Atmos. Ocean Tech., 18, 1171–1183, 2001.

Portabella, M., Stoffelen, Verhoef, A., and Verspeek, J.: A new method for improving scatterometer wind quality control, IEEE T. Geosci. Remote Sens., 9, 579–583, 2012a.

Portabella, M., Stoffelen, A., Lin, W., Turiel, A., Verhoef, A., Verspeek, J., and Ballabrera, J.: Rain effects on ASCAT wind retrieval: Towards an improved quality control, IEEE T. Geosci. Remote Sens., 50, 2495–2506, 2012b.

Stiles, B. W., Pollard, B. D., and Dunbar, R. S.: Direction interval retrieval with thresholded nudging: A method for improving the accuracy of QuikSCAT winds, IEEE T. Geosci. Remote Sens., 40, 79–89, 2002.

Stoffelen, A. and Anderson, D.: Scatterometer data interpretation: measurement space and inversion, J. Atmos. Ocean. Tech., 14, 1298–1313, 1997.

Stoffelen, A. and Portabella, M.: On Bayesian scatterometer wind inversion, IEEE T. Geosci. Remote Sens., 44, 1523–1533, 2006.

Verhoef, A., Portabella, M., Stoffelen, A., and Hersbach, H.: CMOD5.n- the CMOD5 GMF for neutral winds, Ocean and Sea Ice SAF Technical Note, SAF/OSI/CDOP/KNMI/TEC/TN/ 165 v.1, May 2008.

Vogelzang, J., Stoffelen, A., Verhoef, A., De Vries, J., and Bonekamp, H.: Validation of two-dimensional variational ambiguity removal on SeaWinds scatterometer data, J. Atmos. Ocean. Tech., 26, 1229–1245, 2009.

**Table 1.** The percentage of triplets which rejected high-rank solutions are selected by the AR module.

| Wind speed ($m\,s^{-1}$) | | $4 < v \leq 6$ | $6 < v \leq 10$ | $v > 10$ |
|---|---|---|---|---|
| WVC number 1 | Rain free | 0.3 | 0.07 | 0.07 |
| | Rainy | 5.3 | 3.6 | 3.9 |
| WVC number 41 | Rain free | 2.2 | 0.5 | 0 |
| | Rainy | 11.2 | 6.9 | 3.2 |





AMTD
5, 8839–8857, 2012

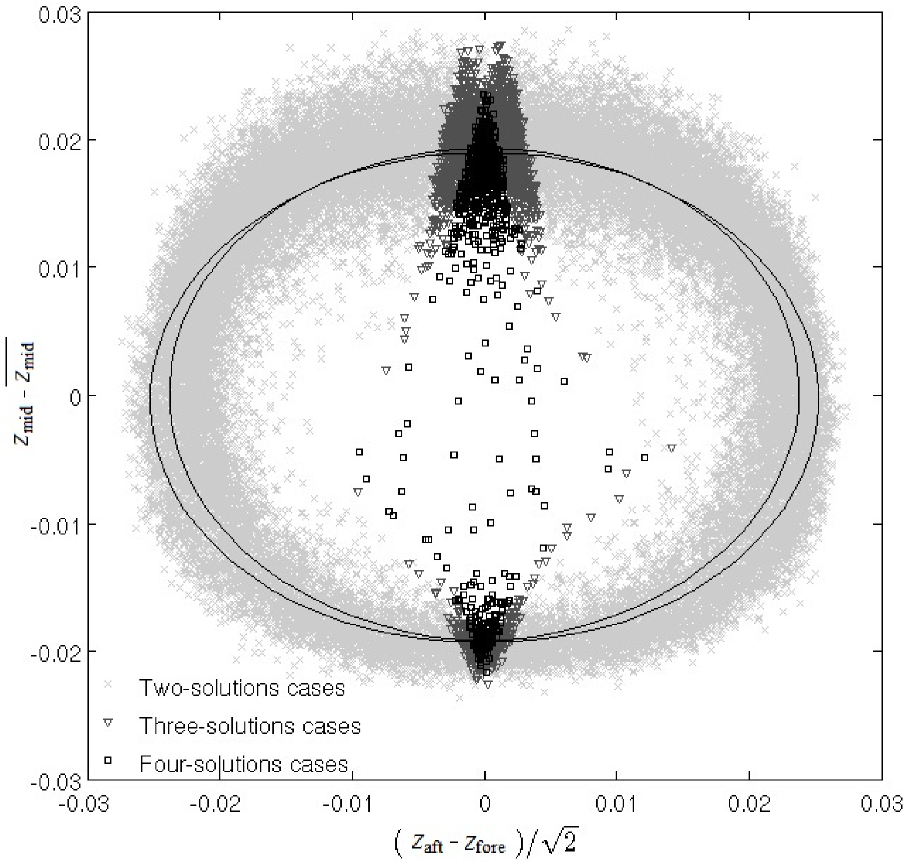


**Fig. 1.** Intersection of the cone with plane $z_{fore} + z_{aft} = 2z_{ref}$ for WVC number 1, for a value of $z_{ref}$ corresponding approximately to a speed of $8\,\mathrm{m\,s^{-1}}$. Triplets within a distance of $\pm 0.01 z_{ref}$ from the mentioned plane are plotted. The cross-, triangular- and square-markers in different gray scale represent the triplets with 2, 3 and 4 wind solutions, respectively.





AMTD
5, 8839–8857, 2012

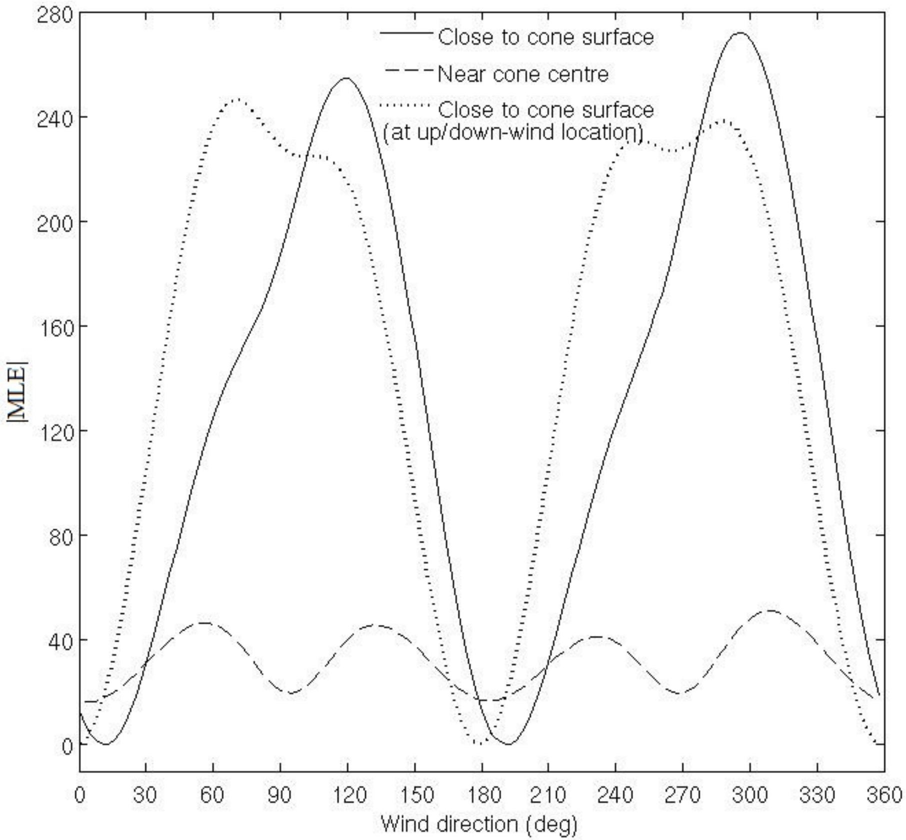


**Fig. 2.** Illustration of the |MLE| versus wind direction during the wind retrieval for three typical cases: triplet close to the cone surface (solid line), triplet near cone centre (dash line), and triplet close to cone surface at up-/down-wind location.





AMTD
5, 8839–8857, 2012

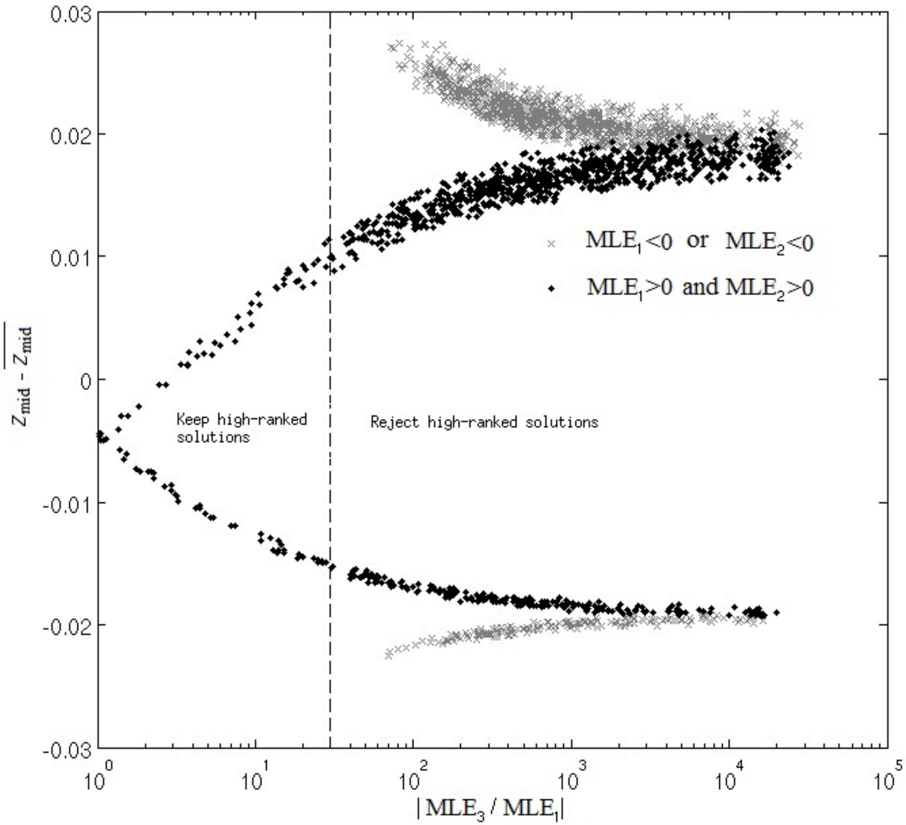


**Fig. 3.** Illustration of the ratio $|MLE_3/MLE_1|$ against the vertical triplet position in Fig. 1 for triplets with more than two solutions. The dashed line indicates the threshold used to separate triplets with high-rank solutions rejected (right side) from those with high-rank solutions kept (left side).





AMTD
5, 8839–8857, 2012

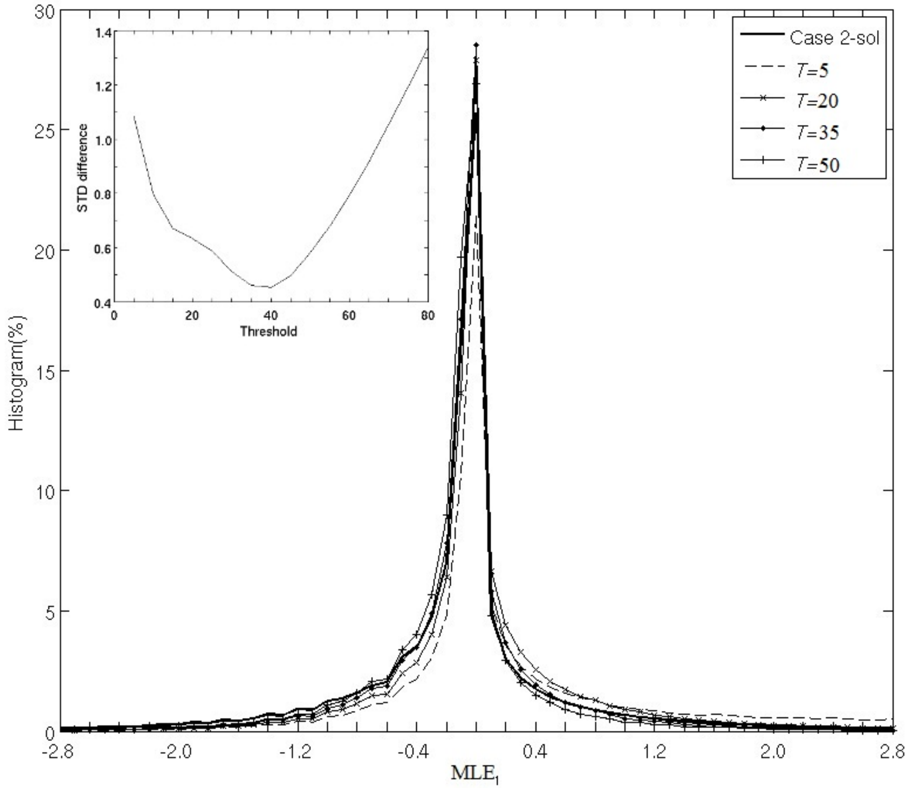


**Fig. 4.** Histogram of the first ranked MLE for two-solution cases (solid line) and high-rank rejected cases for different thresholds. The standard deviation between the histogram of the two-solution cases and that of the high-rank rejected cases is illustrated as a function of the threshold in the upper corner of this figure.

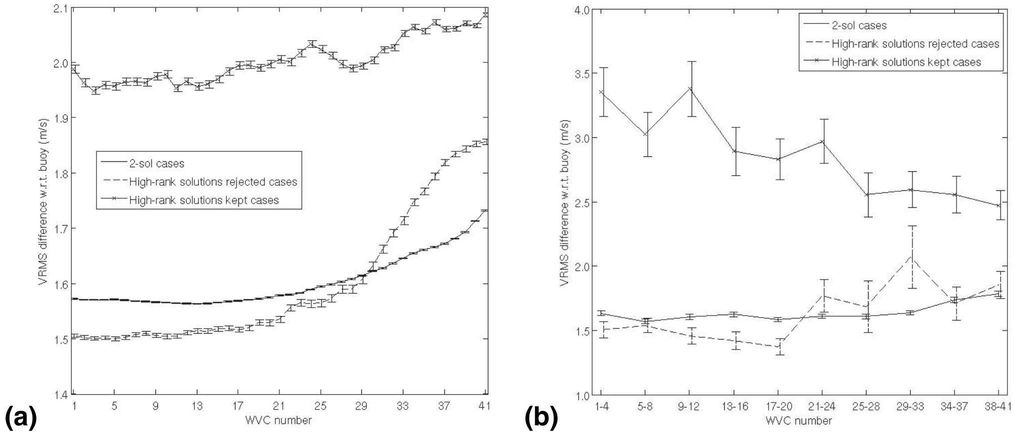


**Fig. 5.** The mean VRMS difference w.r.t. **(a)** ECMWF winds and **(b)** buoy winds as a function of WVC number. Solid line indicates the result of two solutions cases, dash line presents the result of cases with high-rank solutions rejected with threshold $T = 40$, and cross-marked line illustrates the result of cases with high-rank solutions kept. Marker "**I**" denotes the uncertainty bar of the estimated mean VRMS for each WVC bin.





AMTD
5, 8839–8857, 2012